Wind during terrestrial laser scanning of trees: Simulation-based assessment of effects on point cloud features and leaf-wood classification

William Albert[1], Hannah Weiser[1,2], Ronald Tabernig[1,2], Bernhard Höfle[1,2]

[1] 3DGeo Research Group, Institute of Geography, Heidelberg University - (albert, h.weiser, ronald.tabernig, hoelfe)@uni-heidelberg.de
[2] Interdisciplinary Center for Scientific Computing (IWR), Heidelberg University

Keywords: Point Cloud Features, Random Forest, Synthetic Data, Wind-Induced Motion, LiDAR, Leaf-Wood Classification

Abstract

LiDAR point cloud data of trees is often affected by wind-induced movements. This leads to misalignments between overlapping point clouds and distortions in the merged representation. Understanding these wind effects is crucial since they affect downstream tasks like tree parameter quantification and leaf-wood separation. In this study, we investigate the impact of wind during multi-station Terrestrial Laser Scanning (TLS) acquisition on tree structure and leaf-wood classification by simulating TLS acquisitions of trees in both static and windy conditions using the LiDAR simulator HELIOS++. To assess wind effects, we compare the geometric features of leaf and wood points in each scenario and validate our simulations with real tree point clouds acquired in windy conditions. Finally, we train a Random Forest classifier for leaf-wood segmentation on both static and dynamic data and evaluate their performance on both datasets. Our results highlight that two of the nine geometric features are statistically significant in differentiating leaf and wood in windy conditions, compared to six features in static conditions. When trained with static data, leaf-wood classification results drop by ca. 10% intersection over union and decrease by ca. 4% overall accuracy from static to dynamic conditions. Further, we demonstrate that increasing the number of scan positions (i.e. from using one to merging 6 point clouds per tree) reduces classification success by ca. 25% in static conditions and ca. 35% in windy conditions. Our findings emphasize the need to account for wind effects in leaf-wood classification. We show that training on dynamic data can slightly improve classification of dynamic data (ca. 2%) compared to training on static data.

1. Introduction

Light Detection And Ranging (LiDAR) technology has become an invaluable tool in forestry research, providing insights into leaf area quantification, biomass estimation, and the detailed analysis of branch structures using Quantitative Structure Models (QSM) (Yun et al., 2016; Lau et al., 2018). However, for these applications, tree point clouds must accurately represent their real-world counterparts. The main assumption for most analyses is that tree point clouds represent static trees, whereas in reality, trees can move during LiDAR acquisition, affecting point cloud quality and downstream tasks. A primary challenge is the distortion and multiple representations of moving parts introduced by wind during data acquisition, which disrupts the reliable characterization of trees (Côté et al., 2011).

Wind effects are especially problematic for the segmentation of leaf and wood points, as the affected point cloud representation makes the separation of these components more difficult. Prior studies (Yun et al., 2016; Yrttimaa et al., 2023; Wilkes et al., 2017) have noted that even moderate winds reduce point cloud quality, hampering leaf-wood classification and branch segmentation. To mitigate this, researchers have typically acquired data in conditions without wind, where conventional denoising can help to remove artifacts from tree movement. Wind speeds as low as $5\,\mathrm{m/s}$, however, still diminish the accuracy of canopy representation, reducing estimates of canopy openness (Seidel et al., 2012).

Addressing these challenges requires a deeper understanding of how wind influences tree point clouds and the accuracy of leaf-wood classification. To our knowledge, there are no dedicated real-world datasets of trees in windy conditions with leaf and wood points accurately segmented. Manual labeling of such point clouds is even more labor-intensive and time-consuming than the ones captured in optimal windless conditions because the representation of the structure of the trees can sometimes be ambiguous. This limits the quantity of data available for studies focusing on leaf-wood segmentation, in particular for data-hungry deep learning approaches.

To enhance the leaf-wood classification results in static conditions, several studies use synthetic data, generating segmented point clouds through Virtual Laser Scanning (VLS) techniques (Moorthy et al., 2019; Li et al., 2024; Esmorís et al., 2024). VLS enables the simulation of various acquisition scenarios, resulting in synthetic datasets. Each point in the synthetic point cloud carries reference information, including instance and semantic labels, transferred from the input scenes. The reference labels provided by this simulated data can then be used for the training of supervised classification tasks. In this study, we couple VLS with dynamic, animated scenes to generate fully labeled datasets for leaf-wood classification for scenarios affected by wind.

We leverage VLS tree point clouds to specifically examine the impact of wind during multi-station Terrestrial Laser Scanning (TLS) acquisition on tree representations. We investigate how wind alters the Geometric Features (GF) of tree point clouds by comparing point clouds acquired in static and windy conditions. Further, we explore how these variations propagate into the separability of leaf and wood in supervised classification. We investigate the effect of wind during TLS acquisition on the relationship between the number of scans capturing a certain tree part and the leaf-wood classification success. This is based on the assumption that an increase in the quantity of points from different scans within a voxel leads to a greater impact of scan mismatch due to wind.

Additionally, we propose an alternative approach for semantic segmentation of leaf and wood to achieve improved results in case of wind-affected datasets.

Two research questions are addressed:

1. How does wind during multi-station TLS data acquisition change the GF of tree point clouds?
2. How are leaf-wood classification results affected by these changes?

We use VLS to assess the impact of wind on the point cloud representation of trees by computing pointwise GF based on the local neighborhoods (Weinmann et al., 2017). These GF are commonly used as handcrafted features in many applications such as leaf-wood classification, highlighting the broad relevance of this study (Moorthy et al., 2019; Vicari et al., 2019; Ma et al., 2016). Further, real point cloud data of trees is used to demonstrate the representativeness of the simulated dynamic point clouds.

2. Dataset

We create five distinct datasets for our analysis, comprising one real-world point cloud and four virtual point clouds. These datasets are used to quantify the difference in GF and to train GF-based Random Forest (RF) models for pointwise leaf-wood classification (Table 1). The *SimPlotStatic* and *SimPlotDyn* datasets have 437 565 and 441 377 points, respectively. For both datasets, the ratio of wood (40.1%) to leaf points (59.9%) is approximately 2 : 3. For the studied branches of *RealDyn*, *SimSingleStatic* and *SimSingleDyn*, each wood-leaf ratio is ca. 1 : 5.

Table 1. Description of data sets used to compute GF and train the RF model

Dataset name	Point cloud source	Max no. of scan pos.
SimSingleStatic	Simulated point cloud of a single tree - same static 3D mesh for all scan positions	8
SimSingleDyn	Simulated point cloud of a single dynamic tree - different 3D mesh for each scan position	8
SimPlotStatic	Simulated point cloud of multiple tree models - same static 3D mesh for all scan positions	9
SimPlotDyn	Simulated point cloud of multiple dynamic tree models - different 3D mesh for each scan position	9
RealDyn	Point cloud from a real tree scanned in windy conditions	10

2.1 Virtual tree models

In order to generate a virtual point cloud, we create a 3D scene with mesh objects. These objects are used as input for the LiDAR simulator. We create five different quaking aspens (*Populus tremuloides*) tree objects with the *Sapling Tree Gen* Blender add-on (Blender Online Community, 2013), which is based on the work of Weber and Penn (1995). Then, we apply lateral wind motions to each tree, with the objective of emulating the movement of trees in strong winds without causing excessive bending (Figure 1b, $wind_{strength} = 1.25$ [unitless] in the *Sapling Tree Gen* Blender add-on). Next, we loop the animation using 10 frames which are automatically taken at equal intervals of 1 second. We export each frame with a Blender add-on (*dyn_b2h*) made for exporting dynamic scenes from Blender to HELIOS++ (Weiser, 2023). Figure 1 shows the exported static and dynamic representation of a tree object. The meshes of the leaf and the wood structure contain the semantic information allowing the LiDAR simulator to create perfectly annotated point clouds.

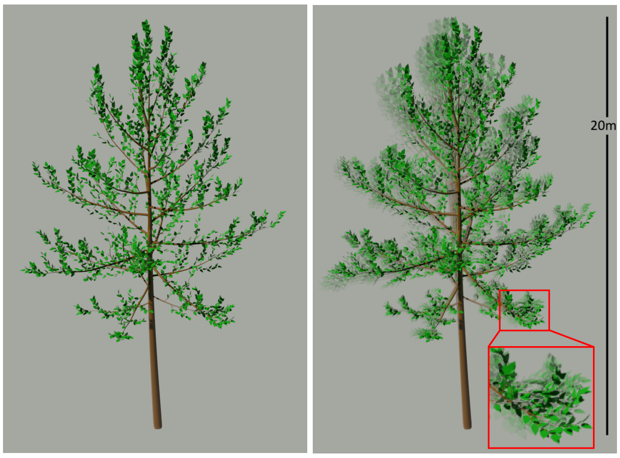

(a) Static tree

(b) Swaying tree - 5 representation merged for visualization

Figure 1. A model of the synthetic tree objects we used for LiDAR simulation colored by leaf (green) and wood (brown). The static tree only contains one object exported from Blender whereas the dynamic one contains five out of ten to show the movement of the tree.

2.2 Virtual laser scanning of static scenes

To provide a precise and automated approach for the VLS-based generation of labeled datasets, we assign a different material property for leaf and wood meshes. Thus, each point is precisely segmented as part of a leaf or wood component, thereby enabling an accurate investigation of wind effects on leaf and wood. We generate the virtual point clouds using the open-source LiDAR simulator HELIOS++ (Winiwarter et al., 2022), requiring objects, a scene in which the objects are positioned, and a survey file indicating the scan settings. For our surveys, we use a RIEGL VZ-400 on a 1.5 m tripod with low resolutions of 0.1° vertically and 0.25° horizontally, and beam divergence of 0.3 mrad. We decided to scan with low resolutions and add more scan positions, as we study the effect of wind on the number of scans per voxel for the classification success.

2.2.1 Single tree In order to better understand the effects of wind during acquisition on the GF of tree point clouds, we perform a branch-to-branch investigation between the static and the dynamic point clouds using one of the five tree models. We assign an ID to five branches at different heights in the tree object to have them already segmented in the output simulated point cloud. The static single tree acquisition is made with eight scan positions in an octagonal configuration circling the same tree object. Point clouds generated from TLS tend to exhibit a lower density of points at the upper part of the canopy. This reduction in point density is primarily due to occlusion effects, where the branches obstruct the laser beam, preventing it from reaching the upper canopy layers effectively (Weiser et al., 2021; Wilkes et al., 2017). Therefore, the distance between the scanner and the tree is established at 18 m, thereby ensuring effective scanning of the top of the crown. The point cloud is then simulated by using the same tree object for each scan.

2.2.2 Group of trees To investigate how wind in trees affects the leaf-wood classification, we create four small plots containing four or five randomly selected different models of quaking aspens (Section 2.1), making a total of 18 trees. Scanning a cluster of trees from eight positions has been proven successful to capture it from all sides (Seidel et al., 2012). Therefore, we scan in a 3×3 grid pattern and place in addition a ninth scanner in the middle of the plot. The distance between the scanners along the grid axis is 12 m. Then, we randomly placed the quaking aspen objects in the plots by scaling them with a ratio from 0.7 to 1.3 and rotating them between 0° and 360° along the z-axis.

2.3 Virtual laser scanning of dynamic scenes

For the purpose of comparing point clouds acquired in static and windy conditions, the aforementioned static scenes are created using a VLS principle of dynamic scenes (Weiser and Höfle, 2024), which is possible with HELIOS++ and the *dyn_b2h* Blender add-on (Winiwarter et al., 2022; Weiser, 2023). The dynamic representation is acquired by scanning different tree frames from each TLS position, described in Section 2.2. Figure 2 shows the acquired static and dynamic point clouds of the single tree acquisition and indicates the identified branches used for further detailed analysis of GF. The same steps are performed to simulate the dynamic version of the plots.

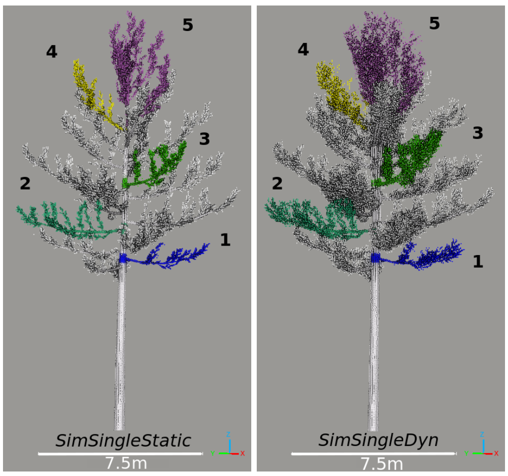

Figure 2. Point cloud representation of the tree in static and windy conditions. The four branches (1-4) and top of the tree (5) are colored in blue, cyan, green, yellow and purple, respectively from bottom to top.

2.4 Real point cloud

The real dataset is a *Tilia cordata* real-world tree point cloud captured in windy conditions in Sandhausen, Germany, with a RIEGL VZ-600i. For the simulated and real point clouds to have an equally low resolution, the real point cloud is downsampled using the timestamp of the points. We use the data of the real tree to corroborate the findings of our experiments conducted on the VLS data. The tree is extracted from a larger point cloud and is scanned from a total of nine positions. We identify three branches A, B and C at respectively 2 m, 4 m and 6 m of height. For each of them, we manually segment the leaf and wood points. Figure 3 shows the tree and the branches alongside their label.

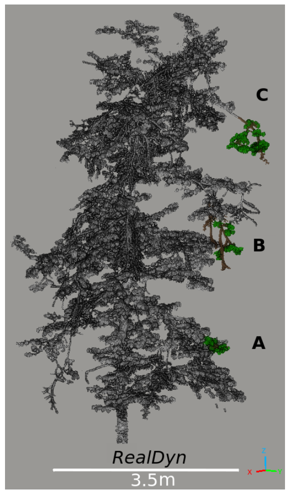

Figure 3. Real-world tree point cloud acquired in windy conditions in Sandhausen, Germany. The three branches of interest are identified as A, B, and C.

3. Methods

The methods employed to address the research questions is summarized in Figure 4 where the portions A and B outlined by the light blue dashed rectangles correspond to Section 3.1 and 3.2, respectively.

3.1 Comparison of the geometric features

To investigate the point distributions in local neighborhoods, we describe the point cloud with representative and significant GF. Moorthy et al. (2019) investigates feature relevance by analyzing leaf-wood classification results from four RF models. It was found that the model from Vicari et al. (2019) delivers the best accuracy and F_1 scores. Therefore, we use the GF from Vicari et al. (2019), which are the three salient features, linearity, eigenentropy and planarity, and we add the three zenith angles of each eigenvector because they vary among trunk, branch, and leaf points in their local neighborhood (Moorthy et al., 2019). In Kumar et al. (2019) it is shown that multiple radii improve the result of the classification compared to considering only a single search radius. As described in Moorthy et al. (2019), opting for the five radii of 0.10 m, 0.25 m, 0.50 m, 0.75 m and 1.00 m is optimal. Indeed, in sparse areas of the point cloud, a search radius less than 0.10 m is not grouping a sufficient amount of point to compute GF. For each dataset, we computed 9 GF from 5 different search radii, for a total of 45 GF using the Jakteristics Python package (Caron, 2020). Table 2 presents the GF alongside their respective description.

To investigate the influence of wind during TLS surveys on the local point distribution of the acquired point cloud, we compare the separability of leaf points to wood points between the branches of interest of *SimSingleStatic* and *SimSingleDyn* datasets. We also compare *SimSingleDyn* with *RealDyn* to investigate the realism of the synthetic dynamic point cloud. The quantitative comparisons are conducted through two

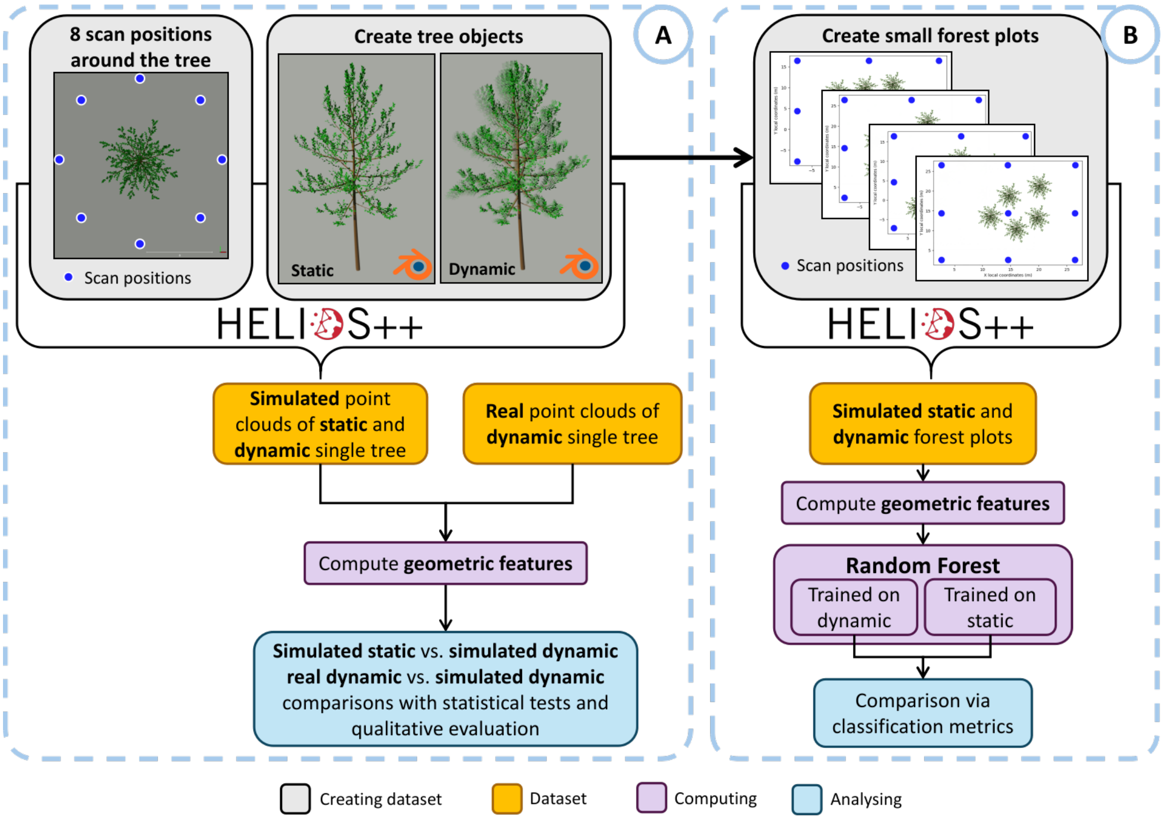

Figure 4. Workflow of this study where dashed rectangles **A** and **B** correspond to Sections 3.1 and 3.2. In **A**, tree objects are created in Blender, scanners are positioned, and HELIOS++ simulation generates datasets (yellow), which are then used to compute geometric features. In **B**, new plots and tree objects are created based on **A**. The simulation with HELIOS++ generates the plots on which geometric features are computed. Two RF models are trained and tested on each plot from which we compare the results.

Table 2. Selected 9 geometric features used to characterize tree point clouds with radii of 0.10, 0.25, 0.50, 0.75 and 1.00 m. The three eigenvalues $\lambda_{0,1,2}$ and the zenith angles of the three eigenvectors $\vec{V}_{0_Z,1_Z,2_Z}$ are sorted from largest to smallest.

Geometric Feature (no.)	Description
Salient features (1,2,3)	$\lambda_2,\ \lambda_0 - \lambda_1,$ $\lambda_1 - \lambda_2$
Linearity (4)	$(\lambda_0 - \lambda_1)/\lambda_0$
Eigenentropy (5)	$-\sum_{n=0}^{2} \lambda_i \cdot \log(\lambda_i)$
Planarity (6)	$(\lambda_1 - \lambda_2)/\lambda_1$
Zenith angles (7,8,9)	$\vec{V}_{0_Z},\ \vec{V}_{1_Z},\ \vec{V}_{2_Z}$

non-parametric statistical tests, namely the Mann-Whitney U (MWU) and the Fligner-Killeen (FK) tests (Mann and Whitney, 1947; Wilcoxon, 1945; Fligner and Killeen, 1976). The tests were selected due to their suitability for independent samples and their robustness to non-normal distributions and presence of outliers, which is the case for our datasets. We chose a conventional significance level of $p < 0.05$ to enable the rejection of the null hypothesis that there will be no statistically significant differences in the separability of leaf and wood in our distributions. MWU compares the distributions of two independent samples to assess whether their medians differ. The FK test evaluates the homogeneity of the variances, i.e. whether the spread of the groups are equal.

We use the MWU test to find which of the GF are the most interesting based on their separability differences and similarities between static and dynamic conditions. We start by computing the GF for *SimSingleStatic* and *SimSingleDyn* datasets. Then, the five branches of interest (cf. Figure 2) are extracted and merged into two distinct static and dynamic point clouds, comprising the full set of branches. We then conduct MWU tests on the merged point clouds to compare the overall tendency of the branches in static and dynamic conditions. From all computed features, we select the eigenentropy and $\vec{V}_{2_Z}$ to be able to show more in-depth results on wind-induced effects.

3.2 Leaf-wood classification

The training and testing of the RF models are performed using the VirtuaLearn3D (VL3D) open-source software (Esmorís et al., 2023). The tuning parameters are set to the default values of VL3D and the GF are computed beforehand and specified in input. Further, we balance the classes by class weighting.

A comparative analysis is conducted to evaluate the performance of two RF models, one trained on static data (static model) and the other on dynamic data (dynamic model). The datasets employed for the training and testing of the models are *SimPlotStatic* and *SimPlotDyn*. Three out of four VLS point clouds of small forest plots (Section 2.2) are used for training and one for testing. To investigate the impact of wind during LiDAR acquisition on the classification of leaf and wood, both models are tested with the two aforementioned datasets. The performances of the models are evaluated using the following metrics: Overall Accuracy (OA), Precision, Recall, F1-score, Matthews Correlation Coefficient (MCC), Kappa and Intersection over Union (IoU).

We also analyze the impact of wind by relating the success and ambiguity of leaf-wood classification to the scanner source count per voxel, using the open-source software VAPC (Tabernig et al., 2024). We assume that the density of points is high enough to compute the GF of each point, even in the voxels with only one scanner source. Next, we investigate the results of the static model tested on the *SimPlotStatic* dataset and the dynamic model tested on the *SimPlotDyn* dataset. The output point clouds from the RF models are first voxelized using edge lengths of 10, 25 and 50 cm. For each voxel, we compute the means of the success rate and class ambiguity. The scanner source count is calculated by retrieving the number of scanners contributing for at least 10% of the points within the voxel. The threshold helps to avoid inflated source counts and get rid of outliers.

4. Results

First, we present the GF calculated for the five tree branches in static and windy conditions, followed by the leaf-wood classification results on the forest plots.

4.1 Geometric features

Three GF separate leaf and wood in both conditions at each radius (λ_2, eigenentropy and $\lambda_0 - \lambda_1$) (Table 3). For $\vec{V_2}_Z$, the small and large search radii significantly differentiate leaf and wood in dynamic and static conditions, respectively. The separability differences on each branch is investigated using the eigenentropy and the $\vec{V_2}_Z$. We selected the eigenentropy as it is significantly separating the leaf from the wood for both static and dynamic conditions. In that case, we can observe if and how the leaf and wood distributions are different in the static and the dynamic conditions. The second GF ($\vec{V_2}_Z$) is selected for comparison of the difference for each branch in both conditions. This selection is made on the basis of its effectiveness to separate leaf and wood in both conditions at 50 cm, when the five branches are merged into a single point cloud.

Table 3. Comparative results of MWU tests for static and dynamic conditions across all GF and radii. Each cell indicates the significance outcome based on p-values: static and dynamic conditions are both significant (SD), are both non-significant (–), only static is significant (S), or only dynamic is significant (D).

Radius	**GF**								
(cm)	λ_2	$\vec{V_0}_Z$	$\vec{V_1}_Z$	$\vec{V_2}_Z$	eigenentropy	linearity	$\lambda_0 - \lambda_1$	$\lambda_1 - \lambda_2$	planarity
10	SD	SD	-	D	SD	S	SD	S	SD
25	SD	SD	S	D	SD	SD	SD	SD	SD
50	SD	S	S	SD	SD	SD	SD	SD	S
75	SD	SD	SD	S	SD	SD	SD	SD	S
100	SD	SD	SD	S	SD	SD	SD	S	SD

For each branch of each dataset, the MWU and FK tests of the eigenentropy with a 0.25 m radius have p-values of 0.00. This indicates that the distributions of the leaf and wood points are statistically different. The violin plots in Figure 5 show the distribution of the normalized eigenentropy (radius = 0.25 m) separated by leaf and wood points for each branch. Comparing the distributions of the synthetic data, branches 1 and 2 are more separable and different in static than in dynamic condition. The separability of branch 3 seems similar, whereas 4 and 5 are more separable in dynamic than in static conditions. In dynamic conditions the top branches demonstrate increased separability, while in static conditions, the reverse is observed. These results are discussed in Section 5.1. Also, the distributions of the *RealDyn* dataset are less smooth, especially for the leaf points. This could be related to the higher complexity of the real point clouds structure compared to the simulated ones.

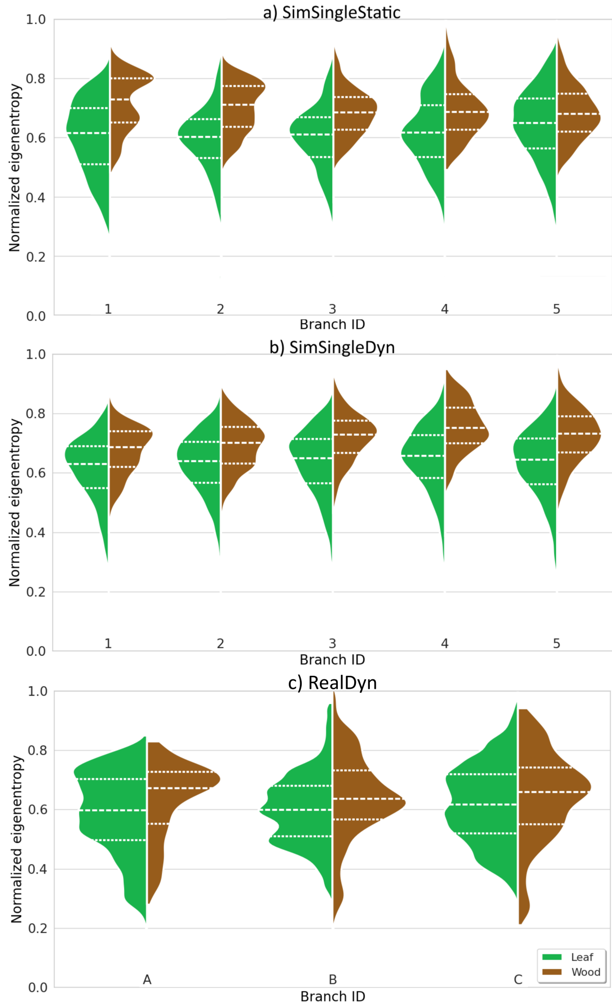

Figure 5. Normalized eigenentropy computed with a 25 cm radius for each branch of the static and dynamic point clouds. The median and quartiles are represented as a central dashed line and dotted lines, respectively.

In the simulated point clouds, the median eigenentropy appears to better differentiate the leaf points from the wood points in the dynamic point cloud. This may be due to the scanner not capturing the small branches with higher branching order in the upper part of the tree. As a result, the main part of the two branches is well represented. Thus, the eigenvalues follow the pattern $0 \approx \lambda_1 \approx \lambda_2 < \lambda_0$, indicating that most of the variations of the points are linear, resulting in a lower eigenentropy. Compared to the wood points in the windy condition, the eigenentropy is higher because of the blurriness of the point cloud. The eigenvalues rather follow the pattern $0 \approx \lambda_2 < \lambda_0 \approx \lambda_1$, meaning the movements caused by the wind introduce more variability, increasing the spatial disorder, and hence the eigenentropy of the wood points. In the real-world point clouds of the branches A, B and C, regions where the point clouds are duplicated and shifted have a higher eigenentropy. These regions are indicated with white rectangles in Figure 6.

Figure 7 shows the point clouds of the synthetic branches 1 and 2 in static and dynamic conditions. The black circles approximately midway along the branch indicate that the

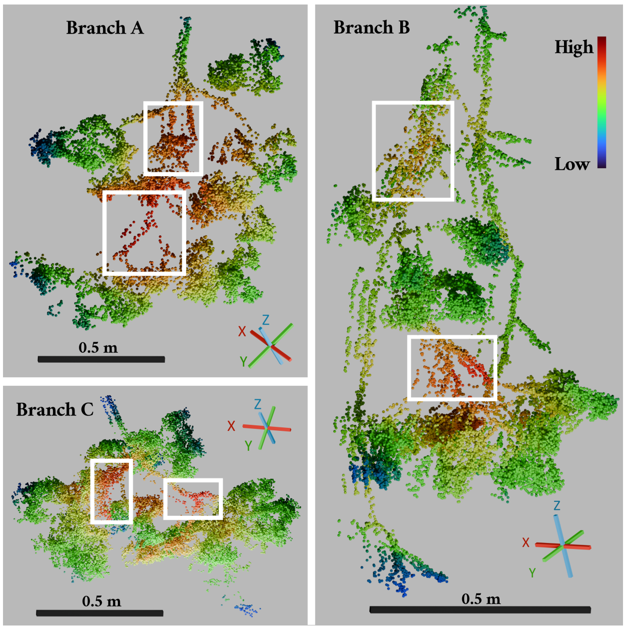

Figure 6. Real branches A, B and C colored by eigenentropy (25 cm search radius).

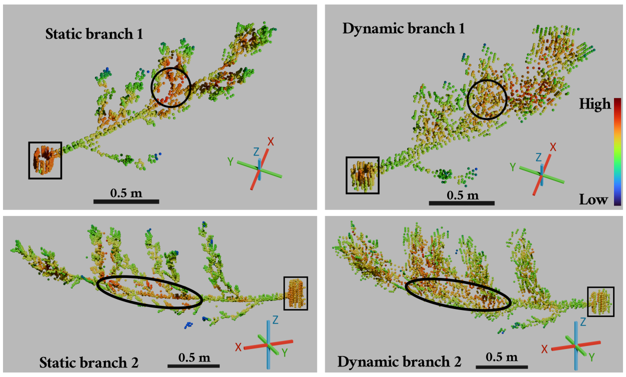

Figure 7. Simulated branches 1 and 2 in static and dynamic scenarios, colored by eigenentropy (25 cm search radius).

dynamic point clouds have a lower eigenentropy than the corresponding static point clouds. This is due to the different curvatures of the branch in each scan. The merged point cloud does not adequately represent the branch object, as the edges and local variations become more diffuse and the randomness of the point cloud increases. This results in a lower eigenentropy. A similar observation can be made for the trunk indicated by the black rectangles in Figure 7. Due to the trunk being more blurred as it moved between scans, the eigenentropy in the dynamic point cloud decreases.

Table 4. MWU test conducted on the $\vec{V}_{2_Z}$ GF (50 cm radius). p-values in bold (> 0.05) indicate no statistical significance between leaf-wood points distribution.

Condition	Branch Id				
	1	2	3	4	5
$\text{Static}_{\text{MWU p-value}}$	0.000	0.000	0.019	**0.077**	0.000
$\text{Dyn}_{\text{MWU p-value}}$	**0.895**	**0.644**	**0.200**	**0.078**	**0.525**

Table 4 shows the MWU p-values for the leaf-wood separability by $\vec{V}_{2_Z}$ computed with a 50 cm radius of the static and dynamic synthetic branches. In this case, the wind has a significant influence on the local point distribution of the branches at mostly each height level within a tree. The p-values are all notably higher in windy conditions, except for branch 4, for which is high in both cases. These high p-values indicate a loss of statistical significance, suggesting that wind has introduced variability in the local point distributions, diminishing the ability to separate leaf and wood points effectively using $\vec{V}_{2_Z}$ as a feature at a branch scale.

4.2 Leaf-wood classification

As described in Section 4.1, the GF are different between the static and dynamic datasets. This section investigates the impact of these differences on leaf-wood classification. Table 5 presents the results of the leaf-wood classifications in descending order of performance. The static model, trained and tested on the *SimPlotStatic* dataset, achieved the highest scores across all metrics with 89.21% OA. These results suggest that the static model is effective when evaluated under similar conditions to its training data. The high MCC and Kappa values further confirm the reliability and consistency of the model on static data. However, when tested on the dynamic data (Table 5, bottom row), which is often the case in real datasets, the results drop by around 5% in each OA, precision, recall, and F1−score and by 8% to 11% for the other metrics. The model trained with dynamic data is therefore better at generalizing, because when tested on the static data, it gets an OA 1.72% lower than the results from the static model and the precision score decreases by less than 1%.

Table 5. Leaf-wood classification results of the RF models both tested on static and dynamic dataset. Highest values for the same prediction dataset are in bold.

Datasets	**Metrics** (%)						
Training - Prediction	OA	P	R	F1	MCC	Kappa	IoU
Static - Static	**89.24**	**89.81**	**87.78**	**88.54**	**79.55**	**77.56**	**77.13**
Dynamic - Static	87.52	88.99	85.35	86.47	76.36	74.25	73.12
Dynamic - Dynamic	**85.30**	**86.29**	**83.14**	**84.11**	**72.83**	**69.36**	**68.43**
Static - Dynamic	84.22	84.76	82.21	83.04	71.25	66.93	66.24

The success of leaf-wood classification varies across different scanner source counts per 25 cm voxels under static and windy conditions. A success rate of 0.5 means that half of the points in the voxel are correctly classified, whereas a class ambiguity of 0.5 means that the model has a 50% chance of correctly classifying the points. Figure 8 indicates that if a location is scanned from more perspectives, the success rate decreases and the class ambiguity increases. Therefore, the classification accuracies are lower. Moreover, this effect is amplified under windy conditions. The black rectangle in Figure 8a may be due to a portion of points where the GF are not computed because of too low point density. Voxels with edge lengths of 10 and 50 cm show consistent results with those of 25 cm, which aims to cover a part of a branch without including other branches. This shows the robustness of the method.

5. Discussion

5.1 Change in distribution of geometric features

From all the GF in this study, we selected the eigenentropy and the $\vec{V}_{2_Z}$ features in order to have a detailed look into the point cloud distribution of the branches. The contrasts between static and dynamic conditions highlight how environmental factors like wind affect the distribution of leaf and wood points. Wind does not significantly reduce the ability of the eigenentropy to distinguish the classes. $\vec{V}_{2_Z}$ is a significant GF for leaf-wood classification in static and dynamic conditions when investigating the full set of five branches. Table 4 shows that

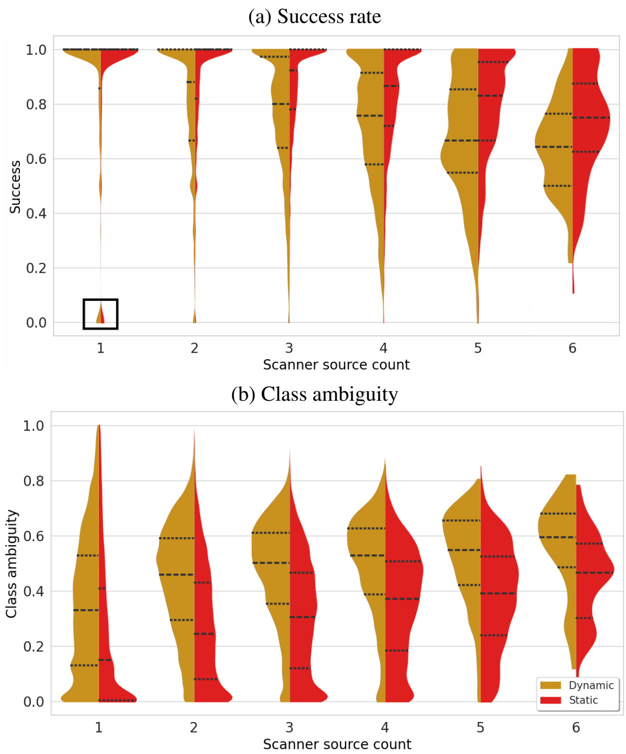

Figure 8. Success rate and class ambiguity of a leaf-wood RF segmentation based on the number of scan source (here equivalent to different scan positions) in 25 cm voxels under static and windy conditions. The black rectangle indicates a portion of points with a null success rate. The median and quartiles are shown as dashed and dotted lines, respectively.

directly transferring a model trained on static data to dynamic data is not feasible with $\vec{V_2}_Z$ due to a low capacity of generalization accross the branches. The differences in separability among the five branches suggest that some are more affected by wind, possibly due to variations in exposure and displacement distances (Dittrich et al., 2017).

5.2 Effects of wind on leaf-wood classification

As noted in Section 4.2, the dynamic model generalizes better, likely because it assigns importance to a broader range of GF, capturing more point cloud variability than the static model. Vicari et al. (2019) found that point cloud sparsity is an obstacle to leaf-wood classification. However, we find that the number of scanner sources per voxel directly influencing results, especially for dynamic data. More scanner sources reduce classification success, highlighting the need to balance scan count and point cloud density and optimize scan positions for effective tree representation. One potential improvement for windy dataset results is to merge the point clouds with similar geometries and discarding the other point clouds to improve representation despite occlusion (Schneider et al., 2019). This approach would benefit cases with many scan positions that lead to redundancies. In such cases, the exclusion of a specific scan would not result in the loss of a significant number of data points.

Future work should explore methods to minimize point cloud shifts in overlapping TLS acquisitions made in strong winds (Wang et al., 2022). One approach could be to shift each scan into a single noiseless merged point cloud by applying local non-rigid 3D transformations. Deep learning could be promising for this task, though requiring substantial training data. For this, the simulated data of dynamic 3D scenes would represent a valuable approach (Weiser and Höfle, 2024). Effective leaf-wood classification of swaying trees would provide crucial information to perform adequate corrections to windy point clouds. Consequently, the biomass estimation, leaf area quantification, or QSM analysis could be performed on wind-affected point clouds after wind corrections.

5.3 Strengths and limitations of synthetic data

The use of synthetic data allows for precise control over variables, including tree structure, wind intensity and LiDAR acquisition settings, thereby enabling targeted studies on specific influences. To test the generalization to real world data, this study should be extended to larger VLS datasets of diverse scenarios. These scenarios should cover different tree species, point cloud resolutions, scanner models and acquisition settings. While the *Sapling Tree Gen* Blender add-on allows to generate diverse tree morphologies, simulating different sizes, shapes, and branch structures, the models can be simplistic in their representations (Bornand et al., 2024). Also, our LiDAR simulations consider tree movements between scan positions and are based on the assumption that the movements of trees during a single scan is negligible. In the future, the movement effects on single scans (e.g., distortions) should be considered by performing VLS on fully animated scenes (Weiser and Höfle, 2024).

6. Conclusion

In this study, we investigate the effects of wind during multi-station TLS acquisitions on local tree point cloud structure and leaf-wood classification, using simulated datasets and a real-world tree point cloud. By using LiDAR simulation, we can fully control the wind influence and the acquisition settings to have perfect annotation reference. The results of our study confirm and quantify the significant impact of wind on how geometric features describe leaf and wood points. Some of the key features (e.g. second and third salient features, linearity, planarity and $\vec{V_2}_Z$) used for leaf-wood classification in the static condition are no longer able to significantly distinguish between the leaf and the wood in windy conditions. Moreover, the capacity of generalization of the random forest model to point clouds affected by wind is better when trained on the dynamic dataset rather than the static dataset. We conclude that labeled point clouds under windy conditions should be also considered for training of machine learning methods. Further research on the specific influences of wind concerning the differences of movements between the lower and the upper part of the trees, optimization of point cloud merging before the leaf-wood classification, and wind corrections will be crucial to improve the accuracy and reliability of separability assessments.

Acknowledgements

This research was funded by the Deutsche Forschungsgemeinschaft (DFG, German Research Foundation) – no. 496418931 (VirtuaLearn3D), no. 411263134 (SYSSIFOSS), no. 528521476 (Fostering a community-driven and sustainable HELIOS++ scientific software) and no. 535733258 (Extract4D project). This work is funded by the BMBF AIMon 5.0: Project no. 02WDG1696. The Federal Ministry of Education and Research (BMBF) is funding the AIMon 5.0 project within the funding measure 'Digital GreenTech – Environmental Engineering meets Digitalisation' as part of the 'Research for Sustainability (FONA) Strategy'.

References

Blender Online Community, 2013. Sapling tree gen. docs.blender.org/manual/en/4.1//addons/add_curve/sapling.html, (last acc: 10.09.2024).

Bornand, A., Abegg, M., Morsdorf, F., Rehush, N., 2024. Completing 3D point clouds of individual trees using deep learning. *Methods in Ecology and Evolution*, n/a(n/a). doi.org/10.1111/2041-210X.14412.

Caron, D., 2020. Jakteristics. github.com/jakarto3d/jakteristics, (last acc: 20.10.2024).

Côté, J.-F., Fournier, R. A., Egli, R., 2011. An architectural model of trees to estimate forest structural attributes using terrestrial LiDAR. *Environmental Modelling Software*, 26(6), 761-777. doi.org/10.1016/j.envsoft.2010.12.008.

Dittrich, A., Weinmann, M., Hinz, S., 2017. Analytical and numerical investigations on the accuracy and robustness of geometric features extracted from 3D point cloud data. *ISPRS Journal of Photogrammetry and Remote Sensing*, 126, 195-208.

Esmorís, A. M., Weiser, H., Höfle, B., 2023. VirtuaLearn3D (VL3D) framework for artificial intelligence applied to point-wise tasks in 3D point clouds. github.com/3dgeo-heidelberg/virtualearn3d, (last acc: 28.10.2024).

Esmorís, A. M., Weiser, H., Winiwarter, L., Cabaleiro, J. C., Höfle, B., 2024. Deep learning with simulated laser scanning data for 3D point cloud classification. *ISPRS Journal of Photogrammetry and Remote Sensing*, 215, 192-213. doi.org/10.1016/j.isprsjprs.2024.06.018.

Fligner, M. A., Killeen, T. J., 1976. Distribution-Free Two-Sample Tests for Scale. *Journal of the American Statistical Association*, 71(353), 210–213. doi.org/10.2307/2285771.

Kumar, A., Anders, K., Winiwarter, L., Höfle, B., 2019. Feature relevance analysis for 3d point cloud classification using deep learning. *ISPRS Annals*, IV-2/W5, 373–380. 10.5194/isprs-annals-IV-2-W5-373-2019.

Lau, A., Bentley, L. P., Martius, C., Shenkin, A., Bartholomeus, H., Raumonen, P., Malhi, Y., Jackson, T., Herold, M., 2018. Quantifying branch architecture of tropical trees using terrestrial LiDAR and 3D modelling. *Trees*, 32, 1219–1231.

Li, W., Hu, X., Su, Y., Tao, S., Ma, Q., Guo, Q., 2024. A new method for voxel-based modelling of three-dimensional forest scenes with integration of terrestrial and airborne LiDAR data. *Methods ecol. evol.*, 15(3), 569-582. doi.org/10.1111/2041-210X.14290.

Ma, L., Zheng, G., Eitel, J. U. H., Moskal, L. M., He, W., Huang, H., 2016. Improved salient feature-based approach for automatically separating photosynthetic and nonphotosynthetic components within terrestrial lidar point cloud data of forest canopies. *Transactions on Geoscience and Remote Sensing*, 54(2), 679-696.

Mann, H. B., Whitney, D. R., 1947. On a test of whether one of two random variables is stochastically larger than the other. *Annals of Mathematical Statistics*, 18, 50–60.

Moorthy, S., Calders, K., Boni Vicari, M., Verbeeck, H., 2019. Improved supervised learning-based approach for leaf and wood classification from LiDAR point clouds of forests. *Transactions on Geoscience and Remote Sensing*, PP, 1-14.

Schneider, F. D., Kükenbrink, D., Schaepman, M. E., Schimel, D. S., Morsdorf, F., 2019. Quantifying 3D structure and occlusion in dense tropical and temperate forests using close-range LiDAR. *Agricultural and Forest Meteorology*, 268, 249-257. doi.org/10.1016/j.agrformet.2019.01.033.

Seidel, D., Fleck, S., Leuschner, C., 2012. Analyzing forest canopies with ground-based laser scanning: A comparison with hemispherical photography. *Agricultural and Forest Meteorology*, 154-155, 1-8. doi.org/10.1016/j.agrformet.2011.10.006.

Tabernig, R., Albert, W., Weiser, H., Höfle, B., 2024. VAPC - Voxel Analysis for Point Clouds. github.com/3dgeo-heidelberg/vapc, (last acc: 28.10.2024).

Vicari, M. B., Disney, M., Wilkes, P., Burt, A., Calders, K., Woodgate, W., 2019. Leaf and wood classification framework for terrestrial LiDAR point clouds. *Methods ecol. evol.*

Wang, D., Puttonen, E., Casella, E., 2022. PlantMove: A tool for quantifying motion fields of plant movements from point cloud time series. *International Journal of Applied Earth Observation and Geoinformation*, 110, 102781.

Weber, J., Penn, J., 1995. Creation and Rendering of Realistic Trees. *SIGGRAPH conference*, 119–128. doi:10.1145/218380.218427.

Weinmann, M., Jutzi, B., Mallet, C., 2017. Geometric features and their relevance for 3d point cloud classification. *ISPRS Annals*, 4, 157-164.

Weiser, H., 2023. Blender add-on for exporting dynamic/animated scenes from blender to helios++. github.com/3dgeo-heidelberg/dyn_b2h, (last acc: 10.09.2024).

Weiser, H., Höfle, B., 2024. Virtual laser scanning of dynamic scenes (VLS-4D): Current approaches and future perspectives in remote sensing. *eartharxiv*. doi.org/10.31223/X51Q5V.

Weiser, H., Winiwarter, L., Anders, K., Fassnacht, F. E., Höfle, B., 2021. Opaque voxel-based tree models for virtual laser scanning in forestry applications. *Remote Sensing of Environment*, 265, 112641. doi.org/10.1016/j.rse.2021.112641.

Wilcoxon, F., 1945. Individual comparisons by ranking methods. *Biometrics Bulletin*, 1, 80–83.

Wilkes, P., Lau, A., Disney, M., Calders, K., Burt, A., Gonzalez de Tanago, J., Bartholomeus, H., Brede, B., Herold, M., 2017. Data acquisition considerations for Terrestrial Laser Scanning of forest plots. *Remote Sensing of Environment*, 196, 140-153.

Winiwarter, L., Esmorís Pena, A. M., Weiser, H., Anders, K., Martínez Sánchez, J., Searle, M., Höfle, B., 2022. Virtual laser scanning with HELIOS++: A novel take on ray tracing-based simulation of topographic full-waveform 3D laser scanning. *Remote Sensing of Environment*, 269. doi.org/10.1016/j.rse.2021.112772.

Yrttimaa, T., Kankare, V., Luoma, V., Junttila, S., Saarinen, N., Calders, K., Holopainen, M., Hyyppä, J., Vastaranta, M., 2023. A method for identifying and segmenting branches of Scots pine (Pinus sylvestris L.) trees using terrestrial laser scanning. *Forestry*, cpad062.

Yun, T., An, F., Li, W., Sun, Y., Cao, L., Xue, L., 2016. A Novel Approach for Retrieving Tree Leaf Area from Ground-Based LiDAR. *Remote Sensing*, 8(11). 10.3390/rs8110942.